ROM SAF Report 36

An initial assessment of the quality of RO data from PAZ

N E Bowler

Met Office, Exeter, UK

Document Author Table

	Name	Function	Date	Comments
Prepared by:	N E Bowler	ROM SAF Project Team	23 Jun 2020	
Reviewed by:	M Forsythe	Met Office review	27 Jan 2020	
Reviewed by:	J Eyre	Met Office review	08 Feb 2020	
Reviewed by:	S Healy	ROM SAF Science Coordinator	09 Mar 2020	
Approved by:	K B Lauritsen	ROM SAF Project Manager	18 Jun 2020	

Document Change Record

Issue/Revision	Date	By	Description
0.1	14 Jan 2020	NEB	1st draft
0.2	04 Feb 2020	NEB	2nd draft, following Mary's review
0.3	12 Feb 2020	NEB	3rd draft, following John's review
0.4	12 Mar 2020	NEB	4th draft, following Sean's review
1.0	23 Jun 2020	NEB	Final version

ROM SAF

The Radio Occultation Meteorology Satellite Application Facility (ROM SAF) is a decentralised processing centre under EUMETSAT which is responsible for operational processing of radio occultation (RO) data from the Metop and Metop-SG satellites and radio occultation data from other missions. The ROM SAF delivers bending angle, refractivity, temperature, pressure, humidity, and other geophysical variables in near real-time for NWP users, as well as reprocessed Climate Data Records (CDRs) and Interim Climate Data Records (ICDRs) for users requiring a higher degree of homogeneity of the RO data sets. The CDRs and ICDRs are further processed into globally gridded monthly-mean data for use in climate monitoring and climate science applications.

The ROM SAF also maintains the Radio Occultation Processing Package (ROPP) which contains software modules that aid users wishing to process, quality-control and assimilate radio occultation data from any radio occultation mission into NWP and other models.

The ROM SAF Leading Entity is the Danish Meteorological Institute (DMI), with Cooperating Entities: i) European Centre for Medium-Range Weather Forecasts (ECMWF) in Reading, United Kingdom, ii) Institut D'Estudis Espacials de Catalunya (IEEC) in Barcelona, Spain, and iii) Met Office in Exeter, United Kingdom. To get access to our products or to read more about the ROM SAF please go to: https://www.romsaf.org

Intellectual Property Rights

Abstract

The PAZ satellite was launched on 22nd February 2018 into a sun-synchronous polar orbit. This satellite carries a polarimetric instrument for taking radio-occultation measurements of the atmosphere. The instrument, known as ROHPP (Radio Occultations and Heavy Precipitation with PAZ) is a variant of an earlier IGOR (Integrated GPS Occultation Receiver) instrument which has been adapted to measure horizontally and vertically polarised signals. Only one radio-occultation instrument is carried by the satellite, and therefore it is only able to measure setting occultations. Due to the dual-polarisation nature of the instrument, the calculation of bending angles follows a slightly different path from conventional instruments.

Overall the performance of the bending angle data is similar to that from other operational instruments. There are differences for the bending angle data in the troposphere, but this is most likely to be due to differences between processing centres, rather than instrumental differences. The refractivity data above 35 km is more accurate than similar data from FY-3C, even though the bending angle accuracy is similar at these levels. This is believed to be due to differences in the choice of climatology used in the processing.

The data have recently been made available in near-real-time. Due to problems with connection between the satellite to the ground infrastructure, the data is experiencing long delays. Improvements have been made recently, but more work in this area is still needed.

Contents

1 Bending angle evaluation

The PAZ satellite is operated by Hisdesat, and the radio occultation data are downloaded to NOAA's Fairbanks station and then transferred to UCAR (University Corporation for Atmospheric Research) for processing. Past data have been processed by UCAR from the 10th May 2018 onwards, and have been made available on the CDAAC (COSMIC Data Analysis and Archive Center) website. Near-real time GNSS-RO data from the PAZ satellite has been available via the Global Telecommunication System (GTS) since 19th December 2019. To assess the performance of the instrument, data was extracted from CDAAC for between 1 December 2018 and 28th February 2019.

The ROHPP instrument onboard PAZ is intended to measure precipitation by examining the polarisation of the received signal. Measuring the signal due to precipitation has been the subject of an extended study [3] and is not considered here. This report focusses on the conventional bending angle and refractivity statistics. Considerable work has been required to process these data into standard products [5].

1.1 Bias and standard deviation characteristics

Figure 1.1 shows the normalised difference between the bending angle observation and the background forecast from the Met Office's operational global numerical weather prediction (NWP) model. These differences are known as the innovations. The mean and standard deviation are calculated as

$$\mu = \frac{1}{N} \sum_{i=1}^{N} \frac{O_i - B_i}{B_i} \tag{1.1}$$

$$\sigma = \sqrt{\frac{1}{N} \sum_{i=1}^{N} \left(\frac{O_i - B_i}{B_i} - \mu \right)^2} \tag{1.2}$$

where O_i and B_i are the observed and background values for occultation i in the period, and there are N occultations overall. Figure 1.1 compares the statistics of PAZ with FY-3C and with Metop-A. PAZ provides fewer observations than either Metop-A or FY-3C. This is expected, since there is only one receiver onboard the satellite, and it therefore only measures setting occultations. Above 10 km the mean statistics from each satellite are very similar. Below this level PAZ shows a negative value for the mean, FY-3C shows a positive value, and Metop-A is negative above 5 km and positive below. Other satellites processed by UCAR also show a negative mean value in this region, so these differences are likely to be a result of processing differences and not related to the instruments.

Above 35 km the standard deviations of the normalised innovations are smallest for Metop-A, and similar for FY-3C and PAZ. Between 10 km and 35 km PAZ and Metop-A have similar standard deviations with FY-3C larger. Below 10 km PAZ and FY-3C have similar standard deviations, with Metop-A larger.

Figure 1.2 shows the statistics for the normalised innovations for PAZ, before and after various quality-control steps have been applied. Approximately 20% of the data have been flagged as having problems by UCAR. In addition to this a small number of occultations are rejected by the Met Office quality control. The number of observations rejected by the data provider is rather higher than one might hope for, but perhaps illustrates the difficulties in generating bending angles from polarimetric data.
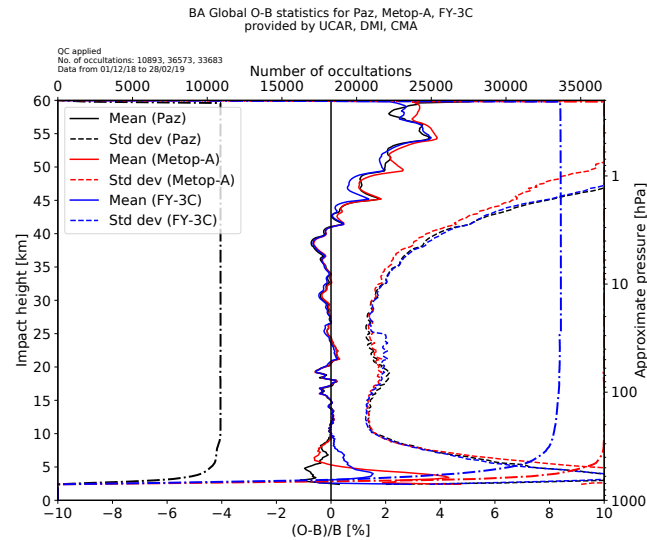
Figure 1.1: The bias and standard deviation of the normalised difference between the observation and the NWP model background forecast $(O-B)/B$ for bending angle. Comparison between statistics for PAZ with Metop-A and FY-3C.
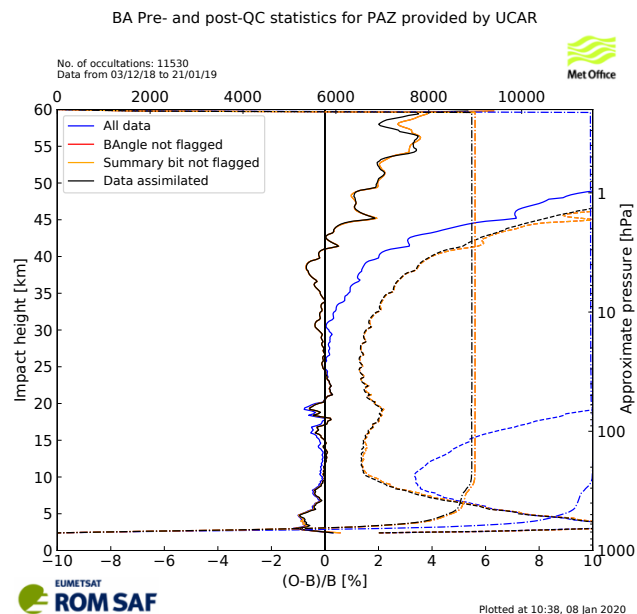

Figure 1.2: The bias and standard deviation of the normalised difference between the observation and the NWP model background forecast $(O-B)/B$ for bending angle. Statistics shown for various points in the quality-control process.
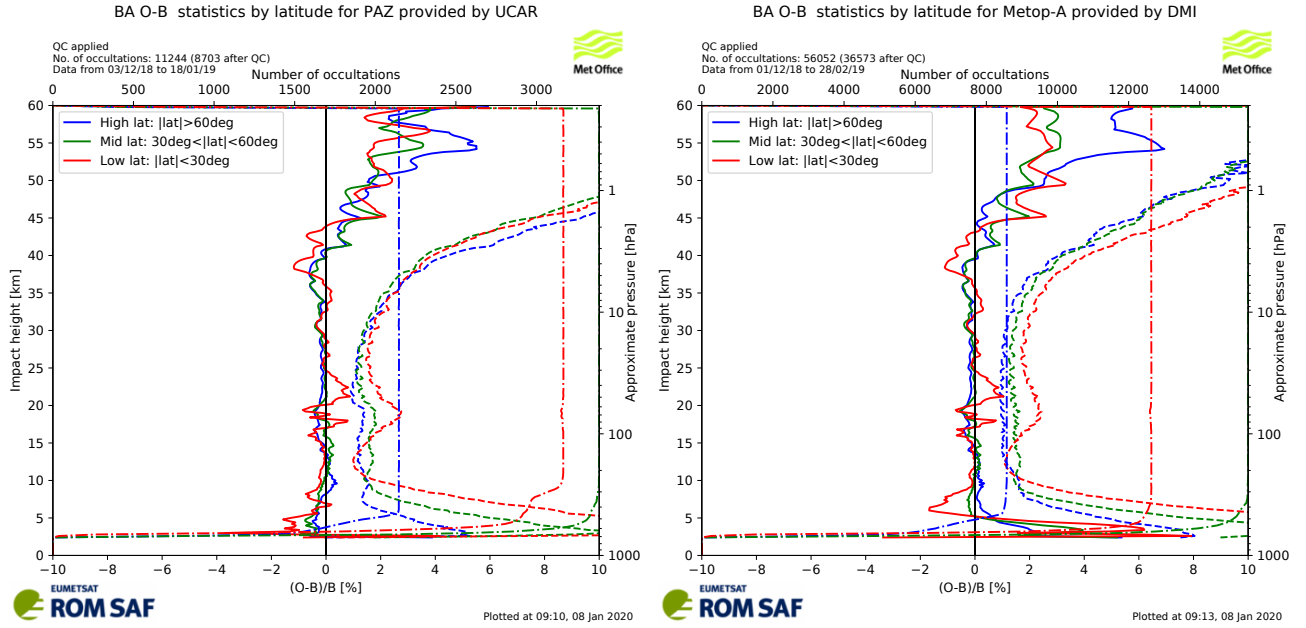
Figure 1.3: The bias and standard deviation of the normalised difference between the observation and the NWP model background forecast $(O - B)/B$, separated by different latitudes for bending angle. Statistics for PAZ (left) and Metop-A (right).

Figure 1.3 shows the bias and standard deviation of the normalised innovations, as Figure 1.1, but separated by different latitude ranges. In the tropical region the standard deviations appear to have a sharper peak in the data for PAZ. Additionally, the standard deviation at high latitudes in the lower stratosphere (7-20 km) appears to be larger for PAZ than Metop-A. This pattern of differences is somewhat similar to that seen for KOMPSAT-5 [1].

1.2 Vertical correlations

When bending angle data is assimilated into the Met Office's NWP system it is assumed that the error in each bending angle measurement is independent of the errors in every other measurement. There-fore we would like the vertical observation-error covariance matrix $\mathbf{R}$ to be diagonal, and the vertical correlations of $O - B$ (which corresponds to the covariance matrix $\mathbf{B} + \mathbf{R}$) to be close to diagonal, containing only the correlations from the background-error covariance matrix. Figure 1.4 shows the vertical correlation of the normalised innovations for PAZ and Metop-A. Due to the way that bending angle is calculated as a smoothed difference between Doppler shifts, we expect a region of positive correlations near the diagonal, and negative correlations at further distances.

The vertical correlations for PAZ are generally somewhat similar to that seen for Metop-A. Above 20 km the core of the positive correlations is broader in the PAZ data than for Metop, indicating that a greater level of vertical smoothing is used for PAZ. Below 20 km there is a sharp decrease in the vertical correlations for PAZ which is not seen in the Metop data. Below 10 km the vertical correlations for Metop data become larger, which is not seen in PAZ data.
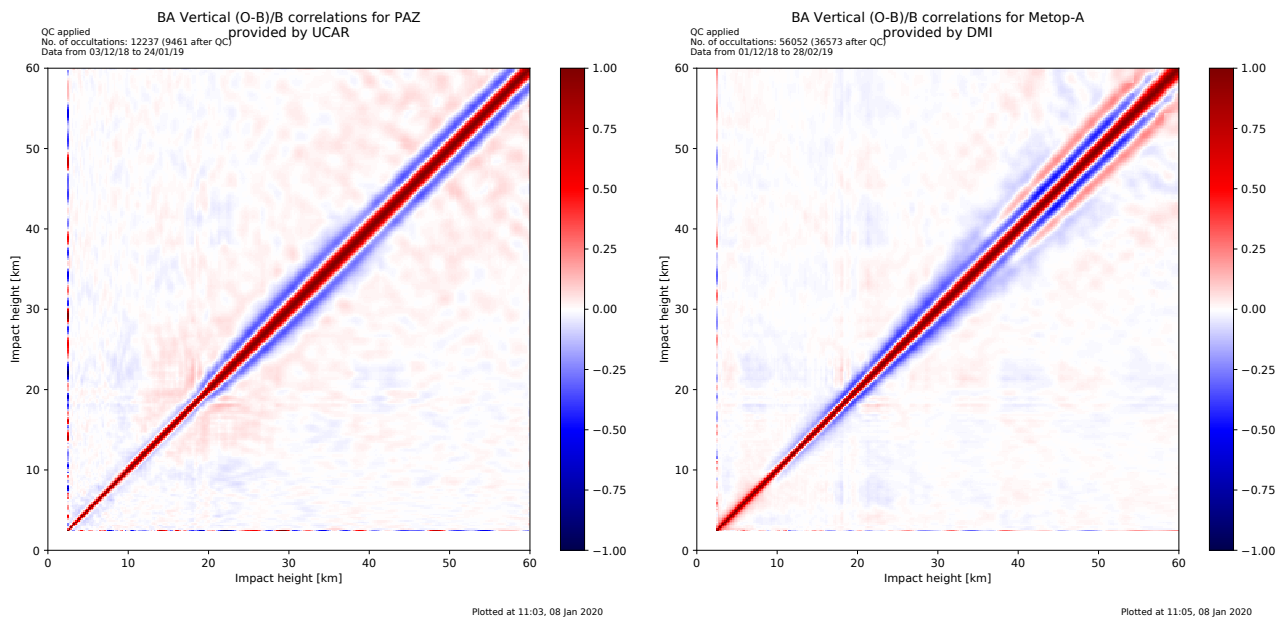
Figure 1.4: Vertical correlations of normalised differences between the observation and the NWP model background for bending angle.

2 Refractivity assessment

Measurements of refractivity are calculated from the bending angle, using an Abel integral and assumptions about the spherical symmetry of the atmosphere. Figure 2.1 shows the mean and standard deviation of normalised differences between the observed refractivity and that produced by the NWP model forecast (i.e. the normalised innovations for refractivity). The mean normalised innovation is very similar between all three satellites between 10 km and 45 km. Above 45 km the mean innovation for FY-3C is larger than for the other two satellites. In the troposphere there are small mean differences between the three satellites, mirroring the differences seen for bending angle.

The standard deviation of the refractivity innovations from PAZ are smaller than those from FY-3C throughout the atmosphere. They are larger than those from Metop-A above 40 km, but are smaller below 10 km. Given that the standard deviations of bending angle innovations above 40 km are similar between PAZ and FY-3C, it is remarkable that the refractivity standard deviations at high levels should be much smaller. This is presumably due to UCAR using a more sophisticated climatology [4] in the statistical opimisation of the refractivity data.

The vertical correlation of the difference between modelled and observed refractivity are shown in Figure 2.2 for PAZ, FY-3C and Metop-A. Since refractivity is derived from the vertical integral of the bending angles, it is expected that there are long-range correlations in this quantity. In the data for Metop-A there are negative correlations off-diagonal around 30 km. A similar region of small correlations is seen in the data for PAZ, but is absent for FY-3C. Above this region all the data are positively correlated, with Metop-A having the smaller long-range correlations. Between 10 km and 20 km the data from PAZ is positively correlated. 20 km corresponds with the point at which the vertical correlations for bending angle showed a sharp increase (Figure 1.4).

The spatial distribution of the average normalised innovation is shown in Figure 2.3 for PAZ and Metop-A. Although the global average of the refractivity difference for PAZ is similar to that for Metop-A (Fig. 2.1) this plot shows that there are large regional differences, particularly around the north pole. Presumably this is driven by the differences in the climatological data used in the statistical optimisation.
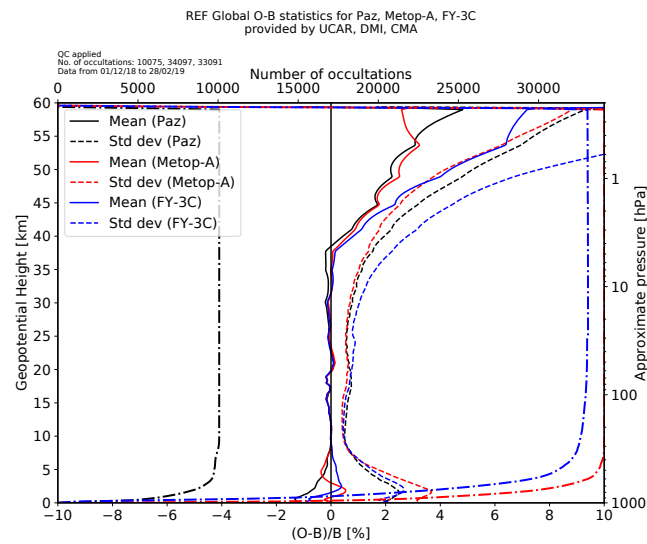
Figure 2.1: The bias and standard deviation of the normalised difference between the observation and the NWP model background forecast $(O - B)/B$ for refractivity.
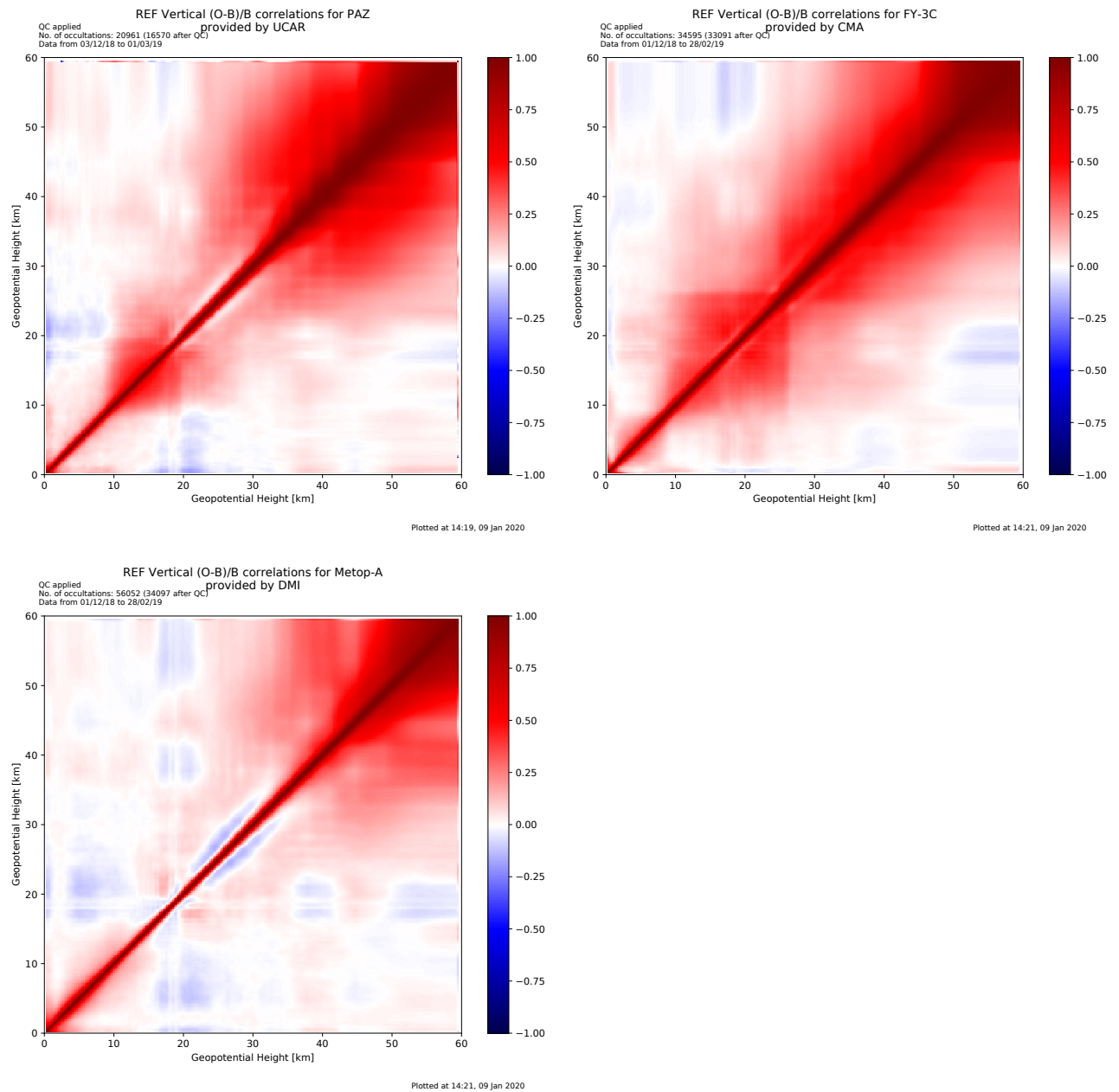
Figure 2.2: Vertical correlations of normalised differences between the observation and the NWP model background for refractivity.
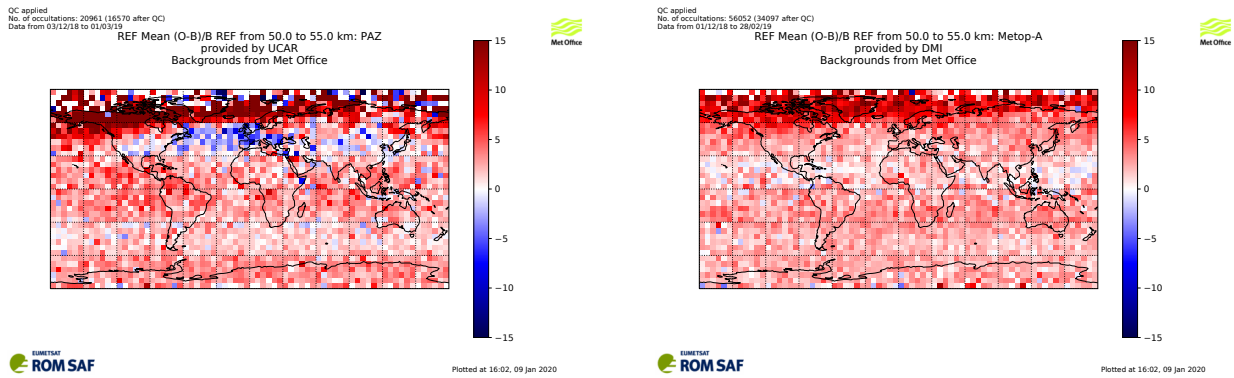
Figure 2.3: The mean value of the normalised difference between the observation and the NWP model background forecast $(O - B)/B$, averaged into 5 degree bins of latitude and longitude.

3 Assimilation test

In order to test the impact that adding these data would have on the operational NWP system an assimilation test was run. This test mimics the operational system at low resolution, adding bending angle observations from PAZ to the data assimilation. Since the test was run on data from the CDAAC archive, all PAZ data were considered for assimilation with no consideration of the timeliness of the data. This is compared with a similar low-resolution run without the additional observations. This run also did not include observations from FY-3D or KOMPSAT, as these satellites have only recently been accepted into operations. The test was run between 1st December 2018 and 28th February 2019 using a global forecast model at N320 resolution (640x480 grid-points). 7-day forecasts are launched every 12h, and these are verified against ECMWF analyses and against observations. Verification results are shown in Figure 3.1. These show that the forecasts which include PAZ observations have smaller errors for many variables. The change appears to be particularly beneficial when verifying against ECMWF analyses. There are no variables for which there is a clear degradation in performance.

It will be noted that these improvements are somewhat similar to those that were seen when introducing observations from FY-3D [2]. Since both satellites provide good quality RO data, it is not a surprise that their impact on the Met Office's NWP system is similar. When verifying impacts using the root-mean-square error (RMSE) as in Figure 3.1 the benefit seen is from a combination of the reduction in bias as well as a reduction in the time-varying forecast errors. To help separate these two, we can examine the impact of the change using the difference in the standard deviation of the forecast error — this is shown in Figure 3.2. Although some of the individual results change, especially for verification against ECMWF analyses, the overall message conclusion that the new observations bring benefit is unchanged.

When assessing forecast performance, we also consider assimilation statistics. This is the root-mean-square (RMS) difference between the forecast from the previous data assimilation cycle (6h ago) and the observations. The change in the RMS difference to satellite sounding channels (microwave and infra-red) provides useful information on the behaviour of the assimilation with the new observations. For this test the change in the RMS difference is generally neutral (with some channels showing a larger RMS difference and some showing a smaller RMS).
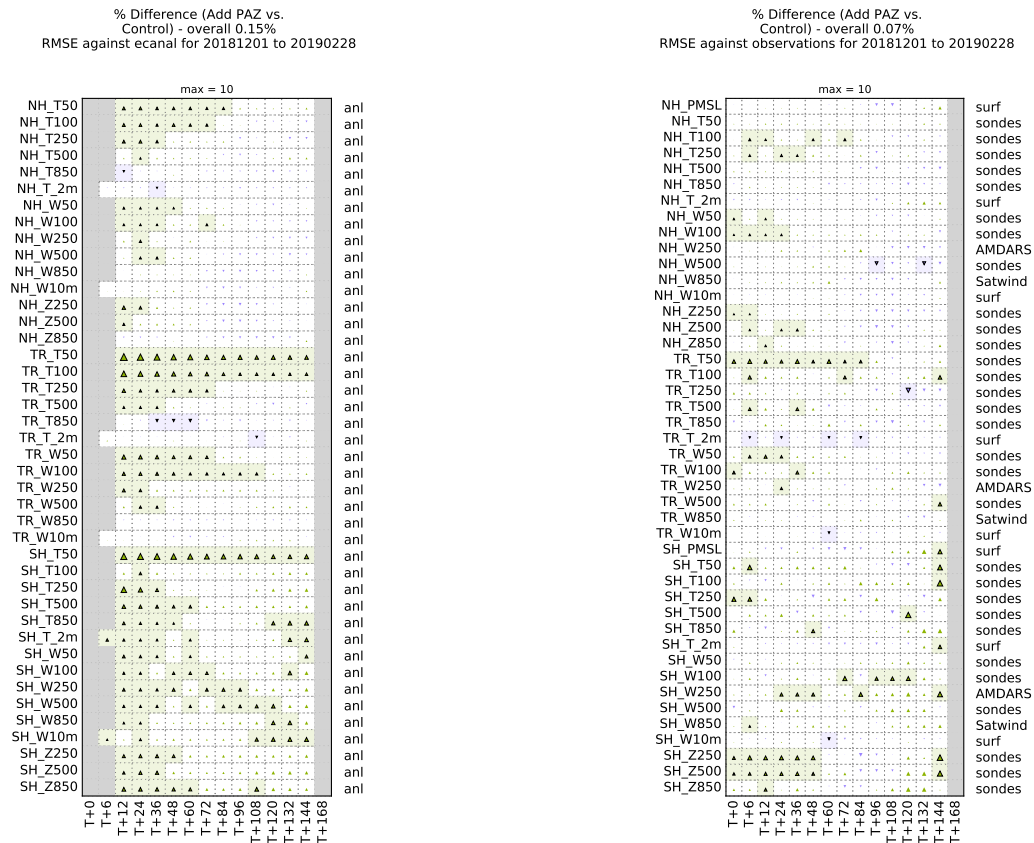
Figure 3.1: Verification results for a test using observations with PAZ, compared to a baseline system using the root-mean-square error (RMSE). (left) Verification against ECMWF analyses and (right) verification against observations. The triangles show the change in the root-mean-square (RMS) error of the forecast, with green (blue) triangles indicating that the test has smaller (larger) errors. Where the change is statistically significant the box surrounding the triangle is shaded.
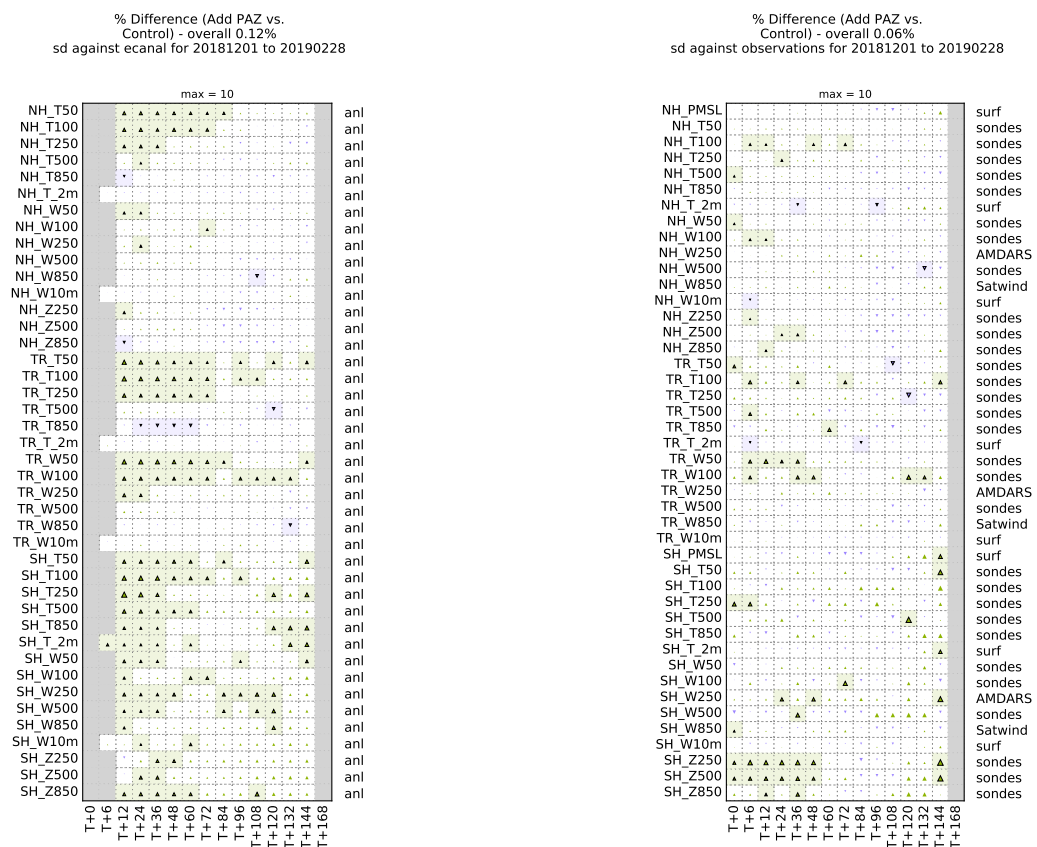
Figure 3.2: Verification results for a test using observations with PAZ, compared to a baseline system using the standard deviation. (left) Verification against ECMWF analyses and (right) verification against observations. Figure format as Figure 3.1

4 Other notable features

The data from PAZ have only been available on the GTS since 19th December 2019. The timeliness of the data, as received via GTS is shown in Figure 4.1. The data is suffering from long delays, and little of the data is being received within three hours. An investigation into the cause of the delays is ongoing, and recent changes by Hisdesat have reduced the delays somewhat. It is understood (E Cardellach, IEEC, personal communication, 2020) that the satellite is unable to make contact with the Fairbanks ground station on every orbit. It is planned to allow PAZ to make use of a second ground station to reduce these problems. The "main" run of the Met Office forecast system takes place at around 2 hours and 42 minutes after the nominal time of the data assimilation window, and the "update" run occurs at approximately 6 hours and 19 minutes after the nominal time. We estimate that approximately 11% of observations from PAZ would be used by the "main" run, and around 36% would be used by the "update" run. Given these low percentages it is not considered that PAZ is ready for use in operational NWP.
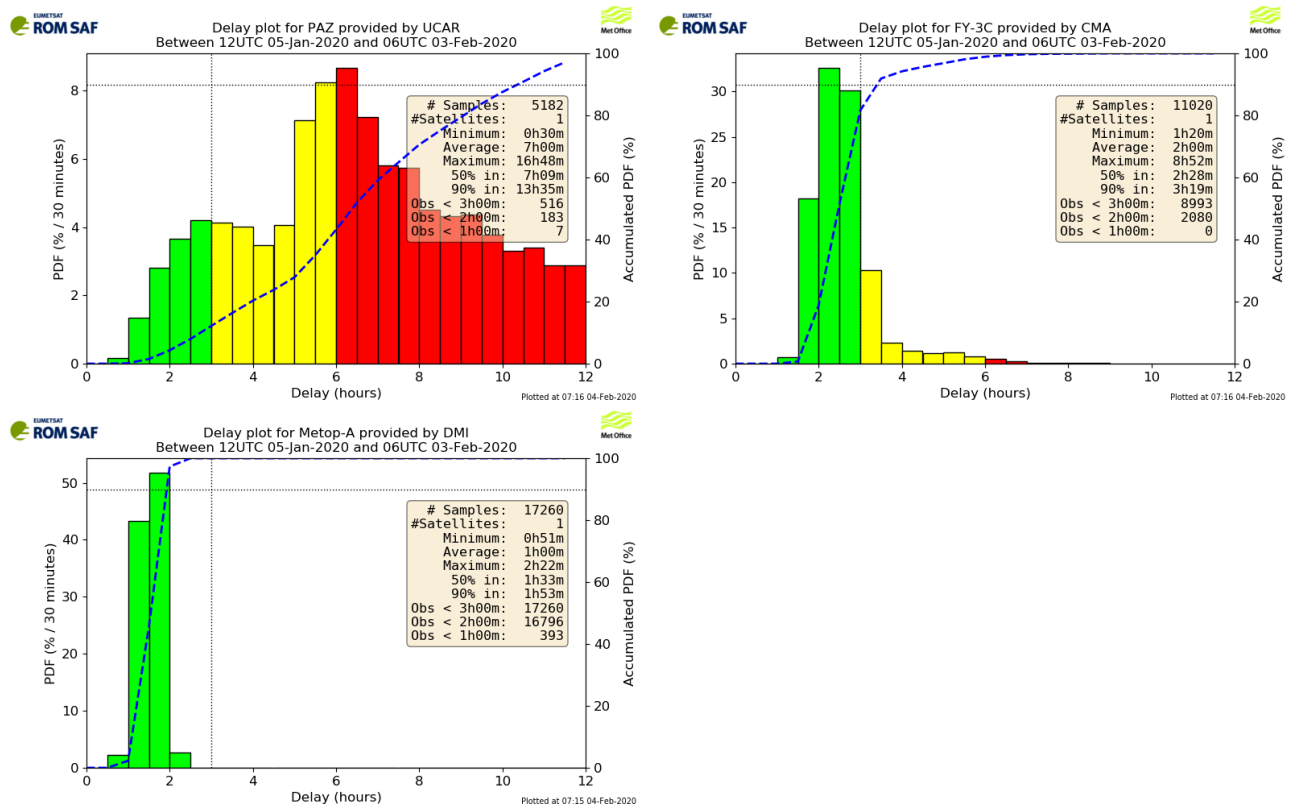
Figure 4.1: Time delay in receiving the occultations, as calculated from the receipt time in the Met Office's observations data base.

5 Conclusion

Archived and near-real-time data from PAZ have been made available to centres around the world. The data are of similar quality to operational satellites. The following list highlights the main differences that are of note:

- The vertical correlations of normalised bending angle innovations are noticeably longer-range above 20 km than below this height.

- The standard deviations of normalised refractivity innovations are clearly smaller than those from FY-3C above 35 km. The standard deviations of bending angle innovations in this height range are similar.

- The normalised refractivity innovations are strongly correlated between 10 km and 20 km.

- NWP trials show small but clear benefit from assimilating bending angles from PAZ.

- The near-real-time data suffers from substantial delays.

ROM SAF (and earlier GRAS SAF) Reports

SAF/GRAS/METO/REP/GSR/001	Mono-dimensional thinning for GPS Radio Occulation
SAF/GRAS/METO/REP/GSR/002	Geodesy calculations in ROPP
SAF/GRAS/METO/REP/GSR/003	ROPP minimiser - minROPP
SAF/GRAS/METO/REP/GSR/004	Error function calculation in ROPP
SAF/GRAS/METO/REP/GSR/005	Refractivity calculations in ROPP
SAF/GRAS/METO/REP/GSR/006	Levenberg-Marquardt minimisation in ROPP
SAF/GRAS/METO/REP/GSR/007	Abel integral calculations in ROPP
SAF/GRAS/METO/REP/GSR/008	ROPP thinner algorithm
SAF/GRAS/METO/REP/GSR/009	Refractivity coefficients used in the assimilation of GPS radio occultation measurements
SAF/GRAS/METO/REP/GSR/010	Latitudinal Binning and Area-Weighted Averaging of Irregularly Distributed Radio Occultation Data
SAF/GRAS/METO/REP/GSR/011	ROPP 1dVar validation
SAF/GRAS/METO/REP/GSR/012	Assimilation of Global Positioning System Radio Occultation Data in the ECMWF ERA-Interim Re-analysis
SAF/GRAS/METO/REP/GSR/013	ROPP PP validation
SAF/ROM/METO/REP/RSR/014	A review of the geodesy calculations in ROPP
SAF/ROM/METO/REP/RSR/015	Improvements to the ROPP refractivity and bending angle operators
SAF/ROM/METO/REP/RSR/016	Simplifying EGM96 undulation calculations in ROPP
SAF/ROM/METO/REP/RSR/017	Simulation of L1 and L2 bending angles with a model ionosphere
SAF/ROM/METO/REP/RSR/018	Single Frequency Radio Occultation Retrievals: Impact on Numerical Weather Prediction
SAF/ROM/METO/REP/RSR/019	Implementation of the ROPP two-dimensional bending angle observation operator in an NWP system
SAF/ROM/METO/REP/RSR/020	Interpolation artefact in ECMWF monthly standard deviation plots
SAF/ROM/METO/REP/RSR/021	5th ROM SAF User Workshop on Applications of GPS radio occultation measurements
SAF/ROM/METO/REP/RSR/022	The use of the GPS radio occultation reflection flag for NWP applications
SAF/ROM/METO/REP/RSR/023	Assessment of a potential reflection flag product
SAF/ROM/METO/REP/RSR/024	The calculation of planetary boundary layer heights in ROPP
SAF/ROM/METO/REP/RSR/025	Survey on user requirements for potential ionospheric products from EPS-SG radio occultation measurements

ROM SAF (and earlier GRAS SAF) Reports (cont.)

SAF/ROM/METO/REP/RSR/026	Estimates of GNSS radio occultation bending angle and refractivity error statistics
SAF/ROM/METO/REP/RSR/027	Recent forecast impact experiments with GPS radio occultation measurements
SAF/ROM/METO/REP/RSR/028	Description of wave optics modelling in ROPP-9 and suggested improvements for ROPP-9.1
SAF/ROM/METO/REP/RSR/029	Testing reprocessed GPS radio occultation datasets in a reanalysis system
SAF/ROM/METO/REP/RSR/030	A first look at the feasibility of assimilating single and dual frequency bending angles
SAF/ROM/METO/REP/RSR/031	Sensitivity of some RO measurements to the shape of the ionospheric electron density profile
SAF/ROM/METO/REP/RSR/032	An initial assessment of the quality of RO data from KOMPSAT-5
SAF/ROM/METO/REP/RSR/033	Some science changes in ROPP-9.1
SAF/ROM/METO/REP/RSR/034	An initial assessment of the quality of RO data from Metop-C
SAF/ROM/METO/REP/RSR/035	An initial assessment of the quality of RO data from FY-3D

ROM SAF Reports are accessible via the ROM SAF website: http://www.romsaf.org

Bibliography

[1] N. E. Bowler. An initial assessment of the quality of RO data from KOMPSAT-5, 2018. ROM SAF report 32, available at https://www.romsaf.org/general-documents/rsr/rsr_32.pdf.

[2] Neill E. Bowler. An initial assessment of the quality of RO data from FY-3D, 2019. ROM SAF report 35, available at https://www.romsaf.org/general-documents/rsr/rsr_35.pdf.

[3] E. Cardellach, S. Oliveras, A. Rius, S. Tomas, C. O. Ao, G. W. Franklin, B. A. Iijima, D. Kuang, T. K. Meehan, R. Padulles, M. de la Torre Juarez, F. J. Turk, D. C. Hunt, W. S. Schreiner, S. V. Sokolovskiy, T. Van Hove, J. P. Weiss, Y. Yoon, Z. Zeng, J. Clapp, W. Xia-Serafino, and F. Cerezo. Sensing Heavy Precipitation With GNSS Polarimetric Radio Occultations. *Geophys Res Lett*, 46:1024–1031, 2019.

[4] M. E. Gorbunov and A. V. Shmakov. Statistically average atmospheric bending angle model based on COSMIC experimental data. *Izvestiya Atmospheric and Oceanic Physics*, 52:622–628, 2016.

[5] D. Hunt. PAZ Neutral Atmosphere Radio Occultation Retrieval Processing. Presentation given at the ROM SAF - IROWG 2019 Workshop, Elsinore, Denmark, 19-25 September 2019, obtainable from https://www.romsaf.org/romsaf-irowg-2019/en/open/1570202090.ca527af47f02b56bd1d9cd50f448ec0d.pdf/Hunt__paz_hv_ro_processing_v03.pdf (last accessed 04 Feb 2020).